The 8th Pacific Rim International Congress on Advanced Materials and Processing
Edited by: Fernand Marquis
TMS (The Minerals, Metals & Materials Society), 2013

SYNTHESIS AND DEPOSITION OF CATALYTIC CeO_2 NANOCRYSTALS VIA AQUEOUS SOLUTION PROCESS

Masakuni Ozawa[a], Katsutoshi Kobayashi[a], Masaaki Haneda[b]

[a] Department of Materials Science and Engineering, EcoTopia Science Institute, Nagoya University
Furo-cho, Chikusa, Nagoya 464-8603, Japan
[b] Advanced Ceramics Research Center, Nagoya Institute of Technology
Asahigaoka, Tajimi, Gifu 507-0071, Japan

Keywords: CeO_2, Nanocrystal, Hydrothermal, Catalyst, Oxygen storage capacity

Introduction

Cerium dioxide (CeO_2, ceria) is one of the important materials in the current many industrial fields such as glass polishing agents, and electrolyte materials of solid oxide fuel cells, three-way catalysts for automobile, as well as medical application (1-5). Physicochemical, electrical and optical applications are expected toward many advanced devices due to versatile properties of CeO_2. Especially, the environmental catalysis using CeO_2 powder materials is widely applied to remove poison gases in automotive engine exhaust. So called oxygen storage capacity (OSC) in three way catalysts (TWC) is one of important functions, in which ceria and its composite catalyst play very important role as oxygen absorption and desorption material. The OSC properties can control the oxygen pressure of exhaust due to fast absorption-desorption reaction of gaseous oxygen into and out from CeO_2, leading to the best performance of noble metal catalyst of TWC. Thus, CeO_2 is very efficient catalyst for the simultaneous elimination of pollutants including CO, HC, and NO in the automotive exhaust gases. Also, the OSC has enhanced removal reaction by oxidation of CO (and hydrocarbons) on CeO_2 to form nonstoichiometric CeO_{2-x}, as following.

$$CeO_2 = CeO_{2-x} + x/2O_{surface} \quad (1)$$
$$CO + O_{surface} = CO_2 \quad (2)$$

The size decrease of CeO_2 increases active surface of catalysis and its reactive rate. Also, recently the particle dimension of nanoparticle is an important factor bringing novel activity as catalysis, which was typically indicated in the case of gold nanocrystal catalyst. (6) Thus, catalytic application of nano-materials in the field of environmental catalytic improvement will be controlled by nanometer-scaled materials from the viewpoint of both simply extremely increasing surface area and novel physicochemical properties. According to this content, CeO_2 nanocrystal has been attractive substance to realize the technological developments in environmental catalyst, and processing to form CeO_2 nanocrystal is a challenging subject. The fabrication of CeO_2 nanoparticles are performed by several methods of hydrothermal and solvothermal treatments (7-13), sol-gel processes (14,15), sonochemical methods (16), microwave heating processes (17), reverse micelle methods (18), and thermal evaporation

methods (19). Also, CeO_2 nanocrystals have shown much morphology such as cubes, octahedrons, wires, and tubes (20-22).

In this study, CeO_2 nanocrystals of around 5 nm in diameter were prepared via aqueous solution process using hydrothermal condition. Then, the structure of CeO_2 nanocrystal by Raman scattering and XRD, and dispersion of deposited nanocrystals in a non-polar solvent were examined. Finally, possible properties of OSC leading to catalytic materials will be described.

Experimental

Synthesis of CeO_2 Nanocrystals

Cerium solution and oleate solution were first prepared by dissolving 7 mmol of diammonium cerium(IV) nitrate ($(NH_4)_2Ce(NO_3)_6$, >95%, Wako Pure Chemical Industries, Ltd.) and 7 mmol of potassium oleate ($C_{33}H_{17}COOK$, 19% solution, Wako Pure Chemical Industries, Ltd.) in 30-mL distilled water, respectively. The oleate solution was added into the cerium solution at room temperature under a vigorously-stirred condition followed by addition of 5 or 10 mL of 25-wt% ammonia aqueous solution (Wako Pure Chemical Industries, Ltd.). The solution mixture containing cerium compounds, oleate salt, ammonia solution was transferred to a Teflon-lined stainless steal autoclave. Subsequently, the sealed autoclave was heated at 150°C or 200°C for 48 hours under a stirred condition at the rate of 800 rpm. After the system was cooled to room temperature under the ambient environment, the precipitates were separated from the solution by centrifugation at 3000 rpm for 30 min. The precipitates containing CeO_2 nanocrystals and oleate salt were then washed with distilled water three times and dried at 90°C for 24 hours in air.

Dispersion of CeO_2 Nanocrystals

Toluene ($C_6H_5CH_3$, >99.5%, Wako Pure Chemical Industries, Ltd.) was selected as a typical non-polar dispersion solvent. The nanocrystals-containing samples, as prepared by mentioned process, were added into toluene and ultrasonically agitated to disperse as solution. After waiting a day for separating supernatant from the excessive precipitation, transparent supernatant which should contain relatively small nanocrystals was extracted. They were further filtrated to remove secondary aggregates and appropriately diluted by adding each solvent for analyses.

The particle-size distribution was measured by the dynamic light scattering (DLS) method using Zetasizer Nano ZS (model ZEN1600, Marvern Instruments Ltd.) for the transparent supernatant solution.

Characterization of solid state of CeO_2 Nanocrystals

A portion of the dried sample without dispersion was characterized by X-ray diffraction (XRD; MiniFlex II, Rigaku) measurement with a monochromator under Cu-$K\alpha$ radiation (λ = 1.5418 Å) at 15 mA and 30 kV. Morphological observation of CeO_2 nanocrystal was carried out with a transmission electron microscope (TEM; JEM2100, JEOL Ltd.) operated at 200 kV. For the observation, toluene dispersion containing CeO_2 nanocrystals was dropped onto a carbon-coated Cu grid (elastic carbon supporting membrane, Okenshoji Co., Ltd.) and evaporated at

room temperature. Elemental analysis was performed by an energy-dispersive X-ray spectroscope (EDX) attached to TEM. Raman spectra were measured with a JASCO NRS-3100 Dispersive Raman Spectrometer, equipped with a TE-cooled charge coupled device (CCD) detector and a green laser (λ=532 nm, frequency-doubled Nd:YVO4, Showa Optronics Co., Ltd.), under the ambient atmosphere. The power of the incident beam on the sample was 6 mW, and the spectral resolution was 0.4 cm^{-1} with the diameter of the analyzed spot being ca. 1 μm. The time of acquisition was adjusted according to the intensity of the Raman scattering. For each sample, the spectra were recorded at several points of the sample (more than five) to ascertain the homogeneity of the sample.

Fundamental catalytic properties (TPR-OSC)

In order to evaluate a fundamental catalytic property, temperature-programmed reduction (TPR) profiles of CeO_2 after heat treatment at 400 °C in air for 1h were obtained using BP-1S (Henmi Co. Ltd., Japan) from room temperature to 400 °C (hold at 400 °C for 20 min) in a 30 $cm^3\ min^{-1}$ flow of 5% H_2/Ar at a heating rate of 10 °C min^{-1}. After the TPR cycle, the flow was switched to Ar and hold for 20min., thereafter, O_2 pulses were injected on the reduced sample at 400 °C, and oxygen storage capacity (OSC) of this material was obtained by calculating the consumption of oxygen as unite of oxygen gas volume per weight of CeO_2. These reactions are described as,

$$CeO_2 + x/2H_2 = CeO_{2-x} + xH_2O \quad \text{(for TPR)} \qquad (3)$$
$$CeO_{2-x} + x/2O_2 = CeO_2 \quad \text{(for } O_2 \text{ pulse)} \qquad (4)$$

Results and discussion

Structure of CeO_2 Nanocrystals

The XRD patterns of the dried sample prepared by the oleate-modified precipitation method (9) followed by the hydrothermal treatment at 150°C and 200°C for 48 hours are shown in **Fig. 1,** indicating the formation of crystalline CeO_2. Crystallite size was briefly estimated to be ~4 nm for CeO_2 from 150°C and ~5 nm from 200°C using three diffraction lines at around 28.3°, 33.0° and 47.4° by Scherrer's equation.

Raman spectroscopy of the as-dried CeO_2 sample (oleate-modified, 200°C) was performed under 5-second-accumulated green-laser irradiation. Strong fluorescence was observed at the beginning of the laser irradiation on the dried sample. Fluorescence basically showed a tendency to decrease with irradiation time due to the burnout of oleate species on CeO_2 surface, which can be caused by laser heating. Finally the fluorescence was almost quenched, maybe because the organic species fully burned out. Under the optical microscopic observation the CeO_2-deposited layer was etched by laser irradiation. After fully hold irradiation, only one peak attributed to triply-degenerated Raman active mode of CeO_2 (cubic fluorite-type) at around 465 cm^{-1} emerged. Such laser irradiated contamination appears in organic materials under lase Raman analysis, however, complete burnout is not so realized in general because of no oxidation phenomenon of organics is assisted by air atmosphere at room temperature. In this study, CeO_2 surface is catalytically active for complete oxidation of organics, because oxygen should be

provided from active surface of nanocrystalline CeO_2. We believe that such complete elimination of surface oleate species in one of the proof to indicate catalytically active property of CeO_2 nanoparticle. In the resultant Raman spectra of CeO_2, the position of the single peak observed in this CeO_2 was deviated to 458 cm^{-1} from 465 cm^{-1} that of bulk CeO_2. The spectrum indicated the same as that of ideal CeO_2 so that CeO_2 nanocrystal with ～5nm in size (from XRD and TEM as described later) has the same symmetry as large crystal. The peak shift is explained by the size effect of small crystal from bulk state. The full width at half maximum (FWHM) of the peak of Raman spectrum was measured as 30 cm^{-1}. Using the peak position and width, the particle size was estimated as 6.6nm (see Ref. 23). The estimated size was almost consistent with that evaluated by XRD.

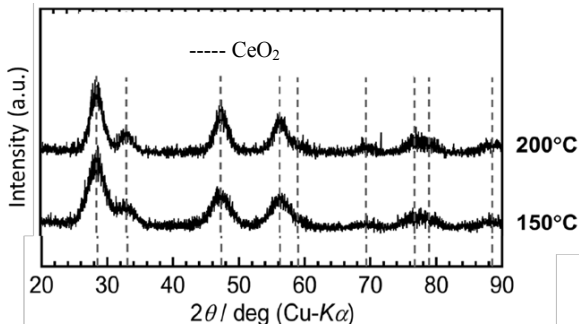

Fig.1 XRD patterns of CeO_2 nanocrystals synthesized with the hydrothermal treatment at 150 ºC and 200 ºC for 48 hours.

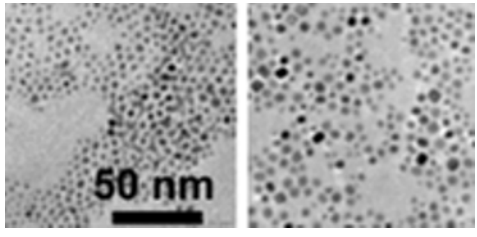

Fig.2 TEM image of CeO_2 nanocrystals synthesized with hydrothermal treatment at 150 ºC (left) and 200 ºC (right) for 48 hours.

Morphology of CeO_2 Nanocrystals

Figure 2 compares low magnification TEM image of the samples synthesized at 150°C and 200°C. The particle-size distribution was in the range of 2-5 nm for at 150°C and 2-7 nm for at 200°C, and the average size was ~3 nm for at 150°C and ~4 nm for at 200°C. Slightly lower average particle size was evaluated with comparison of the crystallite size estimated from the XRD pattern as well as Raman scattering. The particle size from the TEM image indicated that present CeO_2 particles were mainly produced as single crystal with 2-7nm in size with no necking between particles. **Figure 3** shows a magnified TEM which also supported the formation of single-crystalline particles with around 5nm for CeO_2 synthesized at 200°C. Smaller spherical particles and larger polyhedral particles were observed to indicate well-defined nanoparticles with single-crystal polyhedron shape.

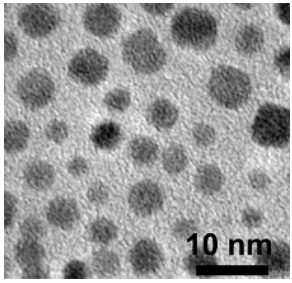

Fig.3 TEM image of CeO_2 nanocrystals synthesized with hydrothermal treatment at 200 ºC.

Dispersion State in Toluene

Transparent dark yellow supernatant solution was formed after the dried samples containing oleate-modified CeO_2 nanocrystals and oleic acid were dispersed in toluene. It indicated the dispersion of CeO_2 nanoparticles without significant aggregation. This dispersion state should be obtained in the synthetic process to provide the narrow size distribution of CeO_2 nanocrystals. The IR spectrum of CeO_2 nanocrystals with oleic acid showed absorption bands at around 400 cm^{-1} and 3000 cm^{-1} which are attributed to the lattice vibration of CeO_2 and the CH_2 or CH_3 vibration from the hydrocarbon chain of oleate species, respectively. Also, the asymmetric and symmetric stretching vibration of the COO- group of oleate species chemisorbed on CeO_2 were detected by IR absorption bands at around 1660-1530 cm^{-1} and at 1440 cm^{-1}. The dispersion state in toluene is due to nonpolar interaction of solvent and surface modified alkyl species absorbed on CeO_2 nanocrystal in solution.

Fundamental catalytic properties (OSC)

The TPR profiles showed a simple curve that the reduction process of CeO_2 with hydrogen started at below 400 ºC and the maximum of the peak will be at higher temperatures than 400 ºC. Actually bulk state CeO_2 has the maximum at around 600 ºC, attributing to the reduction of near surface and lattice oxygen. There will be the lower temperature maxima in the nanocrystalline

CeO_2, however, the surface loss (sintering nanoparticle at low temperatures) due to heat treatment under TPR measurement made it not possible to evaluate characteristics of nanoparticle of CeO_2 in this experiment. Imagawa et al tried to measure OSC of CeO_2 nanoparticles supported by alumina and impregnated by Pt catalyst (24). Our experiments suggest the non-Pt added CeO_2 nanocrystal has also possible as low temperature operating OSC catalyst. The H_2 consumption which started below 400 ºC with reaction of surface oxygen of CeO_2 indicates fast formation of nonstoichiometric CeO_{2-x} due to independent nanocrystalline state. The present CeO_2 nanocrystal will be strongly expected as OSC catalyst as well as advanced functional materials.

Conclusions

CeO_2 nanocrystals were synthesized by the hydrothermal treatment at 150-200°C for 48 hours. The XRD measurement and the TEM observation revealed the formation of CeO_2 nanocrystals with the size of 2-7 nm. Raman scattering suggested the pure CeO_2 structure was stable even in the state of independent nanocrystalline CeO_2. Also, the shift and broadening of Raman scattering was explained by the crytal as size effect in these nanometer region. Dispersion states of the hydrophobic organics-modified CeO_2 nanocrystals were investigated in toluene, leading to formation of clear dispersed colloid solution. Catalytic properties of CeO_2 nanocrystals appeared in the case of laser irradiated burnout of organics on CeO_2 under examination time at laser Raman measurement. Oxygen storage capacity observed at 400°C strongly suggests good oxygen activation of this CeO_2 nanocrystal which is excellent candidate of nanomaterial used as environmental catalytic component.

Acknowledgments

This study was partly supported by Grant-in-Aid for Scientific Research No.25288083 from Japan Society for the Promotion of Science (JSPS).

References

1. E.P. Murray, T. Tsai and S.A. Barnett, *Nature*, **400**, 649 (1999).
2. X.D. Feng, D.C. Sayle, Z.L. Wang, M.S. Paras, B. Santora, A.C. Sutorik, T.X.T. Sayle, Y. Yang, Y. Ding, X.D. Wang and Y.S. Her, *Science*, **312**, 1504 (2006).
3. M.Ozawa, *J.Alloy.Compds.*, **275-277**,886 (1998)
4. R. Di Monte and J. Kaspar, J. Mater. Chem., 15, 633 (2005).
5. Y. Xia, P. Yang, Y. Sun, Y. Wu, B. Mayers, B. Gates, Y. Yin, F. Kim and H. Yan, *Adv. Mater.*, **15**, 353 (2003).
6. T. Ishida, M. Haruta, *Angew. Chem. Int. Ed.* ,**46**, 7154 (2007)
7. Y.C. Zhou and M.N. Rahaman, *J. Mater. Res.*, **8**, 1680 (1993).
8. K.Kobayashi, M.Haneda and M.Ozawa, *Ceramic Trans.*, **239**, 195 (2013)
9. T. Taniguchi, T. Watanabe, N. Sakamoto, N. Matsushita and M. Yoshimura, *Cryst. Growth Des.*, **8**, 3725 (2008).
10. M. Inoue, M. Kimura and T. Inui, *Chem. Commun.*, 957 (1999).

11. S. Yang and L. Gao, *J. Am. Chem. Soc.*, **128**, 9330 (2006).
12. X. Wang and Y. Li, *Chem. Commun.*, 2901 (2007).
13. T.-D. Nguyen and T.-O. Do, *J. Phys. Chem. C*, **113**, 11204 (2009).
14. T. Yu, J. Joo, Y.I. Park and T. Hyeon, *Angew. Chem., Int. Ed.*, **44**, 7411 (2005).
15. M. Niederberger, G. Garnweitner, J. Buha, J. Polleux, J. Ba and N.J. Pinna, *J. Sol-Gel Sci. Technol.*, **40**, 259 (2006).
16. L.X. Yin, Y.Q. Wang, G.S. Pang, Y. Koltypin and A. Gedanken, *J. Colloid Interface Sci.*, **246**, 78 (2002).
17. H. Wang, J.-J. Zhu, J.-M. Zhu, X.-H. Liao, S. Xu, T. Ding and H.-Y. Chen, *Phys. Chem. Chem. Phys.*, **4**, 3794 (2002).
18. T. Masui, K. Fujiwara, K. Machida, G. Adachi, T. Sakata and H. Mori, *Chem. Mater.*, **9**, 2197 (1997).
19. S.G. Kwon and T. Hyeon, *Acc. Chem. Res.*, **41**, 1696 (2008).
20. L. Yan, R. Yu, J. Chen and X. Xing, *Cryst. Growth Des.*, **8**, 1474 (2008).
21. A. Ahniyaz, Y. Sakamoto and L. Bergström, *Cryst. Growth Des.*, **8**, 1798 (2008).
22. C. Tang, Y. Bando, B. Liu and D. Golberg, *Adv. Mater.*, **17**, 3005 (2005).
23. J.E. Spanier, R.D. Robinson, F. Zhang, S.-W. Chan and I.P. Herman, *Phys.Rev.B*, **64**, 245407 (2001).
24. H.Imagawa, A.Suda, K.Yamamura and S.Sun, J. *Phys. Chem. C*, **115**, 1740(2011)